A Novel Motion Control Design Approach Based On Active Disturbance Rejection

Zhiqiang Gao, Shaohua Hu, and Fangjun Jiang
The Applied Control Research Laboratory
Department of Electrical and Computer Engineering
Cleveland State University, Cleveland OH 44115

Abstract: A new digital control solution to motion control problems is proposed. It is based on a unique active disturbance rejection concept, where the disturbances are estimated using an extended state observer (ESO) and compensated in each sampling period. The dynamic compensation reduces the motion system to approximately a double integrator which can be easily controlled using a nonlinear proportional-derivative controller. The proposed Active Disturbance-Rejection Controller (ADRC) consists of the ESO and the nonlinear PD controller and is designed without an explicit mathematical model of the plant. Hence the controller is inherently robust against plant variations. Through simulation, frequency response analysis, and hardware tests, it is shown that the proposed approach is superior to the current PID based technology. It stands out especially in handling set point change, large inertia and friction variations, and external torque disturbance, all of which is seen as "disturbance" by ADRC and is actively compensated. The improvement in transient response and steady state error is also quite evident.

I. Introduction

Motion control applications can be found in almost every sector of industry, from factory automation and robotics to high-tech computer hard-disk drives. They are used to regulate mechanical motions in terms of position, velocity, acceleration and/or to coordinate the motions of multiple axes or machine parts. Similar to other industrial control applications, proportional-integral-derivative (PID) control is the method of choice in most motion applications [1-6]. In applications where frictions are not significant, proportional-derivative (PD) controller are most popular. The PID is simply to use and easy to understand. Over the years, practicing engineers have developed various tuning methods for the ease of application. The frequency response method proves to be very helpful in understanding and analyzing motion control systems.

Productivity and efficiency drive the advance of motion control technology. During the past several years, there have been significant advancements made in the capabilities of microcontrollers and digital signal processors. It is anticipated that these advances will continue at a dramatic rate. We believe that these advances present timely opportunities for implementing new control strategies, which can improve the performance and reliability of motion control systems.

In this paper, we propose a new methodology for motion control applications. It is based upon the recent development in active disturbance-rejection control [7,8]. Through simulation and hardware tests, it was demonstrated that this is a promising new technology. It is a more powerful method than PID and is easy to use. Once it is set up for a class of problems within a fairly wide range of operation, no tuning is needed for start up or changes in the dynamics and/or disturbances. That is, a true turn key operation.

The paper is organized as follows. The motion control problem is introduced in Section II. The general principle and structure of the ADRC is presented in section III. Simulation and hardware tests are shown in section IV and V, respectively. Finally, some concluding remarks are given in Section VI.

II. The Motion Control Problem

2.1 Mathematical Model

In a typical application using a motor as the power source, the equation of motion can be described as:

$$\ddot{y} = f(t, y, \dot{y}, w) + bu \qquad (1)$$

where y is position, u is the motor current, b is the torque constant, and w represents the external disturbance such as vibrations and torque disturbances. The friction, the effect of inertia and various other nonlinearities in a motion system are all represented by the function f(•). Note that f(•) is generally a time-varying function. In most motion control literature, the linear, time-invariant, approximation is used:

$$\ddot{y} = -\frac{c}{J}\dot{y} + \frac{b}{J}u \qquad (2)$$

where J is the total inertia of the motor and load, and c is the viscous friction coefficient. This linear approximation allows the use of the transfer function

$$G(s) = \frac{b}{s(Js + c)} \qquad (3)$$

as a convenient model of the motion system.

2.2 Motion Profiling

An interesting characteristic of motion control is the use of motion profile. Using position control as an example, it is not good enough to just rotate an axis by the desired amount, say one revolution. How it gets there is also relevant. The velocity, acceleration and jerk (differentiation of the acceleration) all play important roles in a motion application and their desired trajectories are known as motion profiles. The motion profile is used as the command input in the closed-loop control, as opposes to

the step command. It's an example of good engineering practice but is seldom addressed in control textbooks.

In this paper, a profile generator is used to produce a position profile, $v_1(t)$, and the velocity profile $v_2(t)$ from the desired set-point of one revolution. For simplicity, the industry standard trapezoid velocity profile, shown in Figure 1, is used.

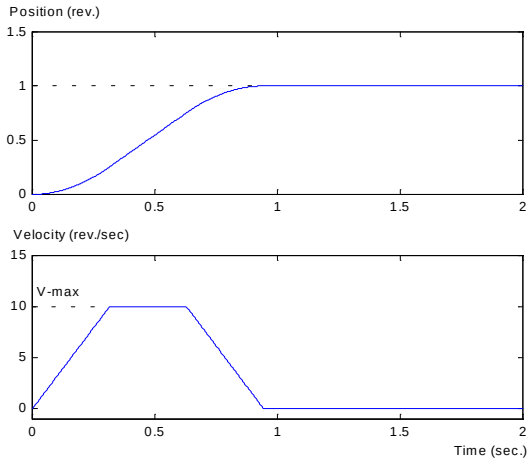

Figure 1 Position and velocity profiles

2.3 The Needs for Improvement

In this paper, we address the following needs for improving the current motion control techniques:

- High performance in terms of forcing the motion variables such as position and velocity to track the desired trajectory quickly and accurately
- High degree of robustness: making the motion control system highly tolerant of dynamic variations such inertia and friction changes
- Better external disturbance rejection capability such as torque disturbance rejection
- Simplify the design process for the users

III. The Active Disturbance-Rejection Controller

The ADRC is based on the idea that in order to formulate a robust control strategy, one should start with the original problem in (1), not its approximations in (2). Although the linear model makes it feasible for us to use the powerful classical control techniques such as frequency response based analysis and design methods, it also limits our options to linear algorithms and makes us overly dependent on the mathematical model of the plant.

3.1 A Time Domain Based Control Concept

Rewrite the original motion equation in state space

$$\begin{cases} \dot{x}_1 = x_2 \\ \dot{x}_2 = f(t, x_1, x_2, w) + bu \\ y = x_1 \end{cases} \quad (4)$$

we propose the following concept: in order to control the system (4), we don't necessarily need the analytical expression of f(•) or it's approximation, as long as we can estimate it closely in real time and make adjustments at each sampling point in a digital controller. A simplistic approach is

$$\hat{f}(t, x_1, x_2, w) = bu - \dot{x}_2 \quad (5)$$

which requires the measurement or estimation of the acceleration, $\dot{x}_2$. A more systematic approach that has been tested successfully in many simulations and hardware is described below.

3.2 The Extended State Observer

The extended state observer (ESO) proposed by Prof. Han [7] is a unique nonlinear observer designed to estimate f(•). First, f(•) is augmented as a state for the system:

$$\begin{cases} \dot{x}_1 = x_2 \\ \dot{x}_2 = x_3 + bu, \;\; x_3(t) \underline{\Delta} f(t, x_1, x_2, w) \\ \dot{x}_3 = h(t) \\ y = x_1 \end{cases} \quad (6)$$

where h(t) is the derivative of f(•) and is unknown. Then, the following nonlinear observer is used to estimate x, and therefore f(•).

$$\begin{cases} \dot{z}_1 = z_2 - \beta_{01} g_1(z_1 - y(t)) \\ \dot{z}_2 = z_3 - \beta_{02} g_2(z_1 - y(t)) + b_0 u \\ \dot{z}_3 = -\beta_{03} g_3(z_1 - y(t)) \end{cases} \quad (7)$$

where β_{01},β_{02} and β_{03} are observer gains and $g_1(.)$, $g_2(.)$ and $g_3(.)$ are appropriate linear or nonlinear functions. An example of such function is

$$g_i(\varepsilon) = fal(\varepsilon, \alpha, \delta) = \begin{cases} |\varepsilon|^{\alpha} sign(\varepsilon), & |\varepsilon| > \delta \\ \dfrac{\varepsilon}{\delta^{1-\alpha}}, & |\varepsilon| \le \delta \end{cases} \quad (8)$$

b_0 in (7) represents the nominal value of the torque constant in (1) and (4), for generality.

Remarks:

1. The use of nonlinear function $g_i(•)$ in (7) can make the observer more efficient. The nonlinear function (8) was selected based on experiments. Intuitively, it is a nonlinear gain function where smaller error corresponds to higher gain. This technique is used widely in industrial applications.
2. If $g_i(•)$ i=1,2 …, are chosen as linear functions, then (7) is equivalent to the well known Luenburger observer found in linear system theory;
3. Similar to linear observers, the observer equation (7) reflects our best knowledge of the system. If we know more about the plant, such as the friction, then it should be incorporated into the observer to make it more efficient.
4. Note that there is a linear segment in (8) in the neighborhood of the origin. It was discovered experimentally that the nonlinear function in (8)

makes the observer converge faster than its linear counterpart and the linear section in (8) makes the output of the observer smoother.

5. The proper selections of the gains and functions in (7) are critical to the success of the observer. One approach is to design the linear observer first and then gradually increase the nonlinearity to improve the performance. It was discovered that once the ESO is properly set up, the performance of the observer is quite insensitive to the plant variations and disturbances.

3.3 The Control Law

The architecture of ADRC is shown in Figure 2. It consists of three components: the Profile Generator, the ESO and the Nonlinear PD. The control law is defined as

$$u(t) = u_0(t) - z_3(t)/b_0 \qquad (9)$$

which reduces the plant to a double integrator, which in turn is controlled by the nonlinear PD controller:

$$u_0(t) = k_P f_1(\varepsilon_1) + k_D f_2(\varepsilon_2) \qquad (10)$$

where $\varepsilon_1 = v_1 - z_1$, $\varepsilon_2 = v_2 - z_2$, are position and velocity error, respectively, k_P and k_D are the gains of the PD controller, and $f_1(\cdot)$ and $f_2(\cdot)$are appropriate nonlinear functions, such as the one in (8).

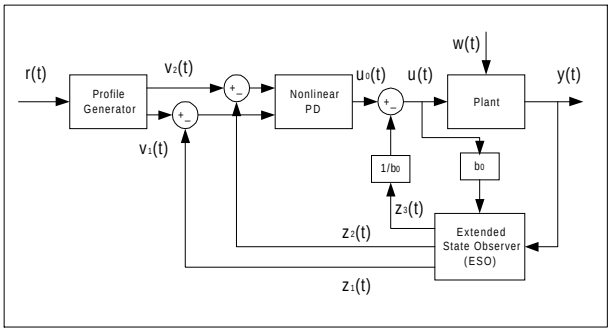

Figure 2 Structure of the Active Disturbance-Rejection controller

Note that the profile generator generates the desired output trajectory, $v_1(t)$, and it's derivative, $v_2(t)$. They are then compared to the filtered output, $z_1(t)$, and its derivative, $z_2(t)$. Clearly, the differentiation of the error is obtained without taking the direct differentiation of the set point or the output. This makes it much less sensitive to noises in the output and discontinuities in the setpoint r(t).

IV. Simulation Study

The proposed motion control approach is first tested in simulation using Matlab/Simulink. The transfer function of the plant takes the form of

$$G(s) = \frac{16.5}{s(0.71s+1)} \qquad (11)$$

This model was derived from a hardware setup that will be used later in experimentation. The controller, in particular the ESO, is digitized using the simple Euler's method, with the sampling rate of 1.0 KHz. The simulation diagram in Simulink of the discrete ADRC system for a DC servo system is shown in Figure 3.

Nominal Response:

The ADRC controller is first tuned experimentally and then compared to a well-tuned PID controller. The trapezoidal profile defined in Figure 1 is used as the target for the position signal, y, to follow. The responses of both systems are shown in Figure 4. Both controllers perform well but ADRC yields smaller error.

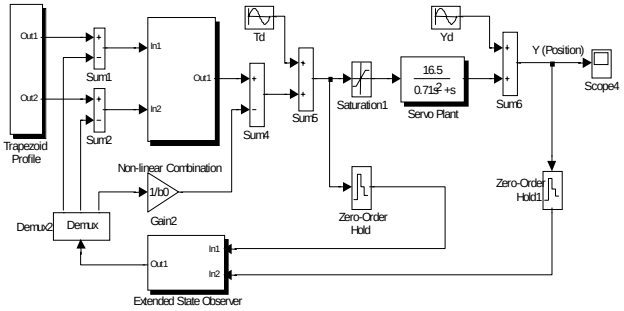

Figure 3. ADRC servo system in Simulink

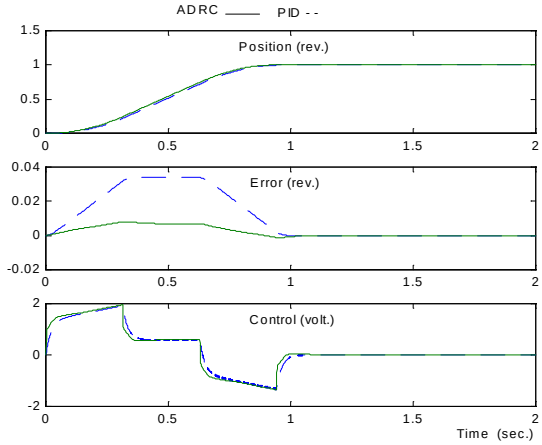

Figure 4 Nominal Responses of ADRC and PID

Robustness and Disturbance Rejection Tests:

To see how robust the ADRC is, we increase the inertia constant J of the plant by 100% and repeat the control simulations without changing any parameters of the ADRC and PID controllers. In hardware testing, the inertia can be changed by adding more weight to the disk. Responses shown in Figure 5 demonstrate a remarkable improvement the ADRC brings. In addition, to test how these systems perform in the presence of external disturbances, a constant torque disturbance is exerted at t= 2.0 second. The magnitude of this disturbance represents 20% of the maximum torque. The responses are shown in Figure 6. Once again, the ADRC performs much better than PID. PID performed poorly in this case because, in order to avoid overshoot, the integral gain used is very small, making it essentially a PD controller. This is quite common in motion applications.

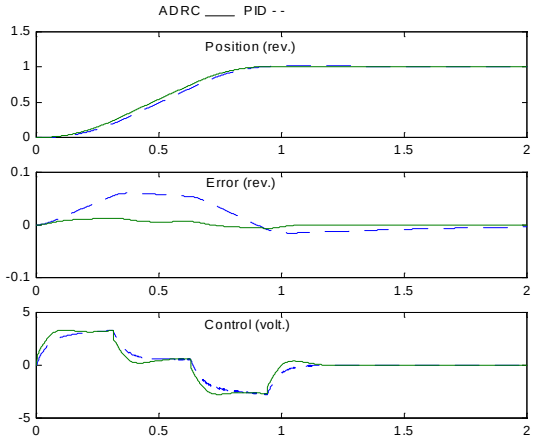

Figure 5 Simulation results with plant inertia increased by 100%

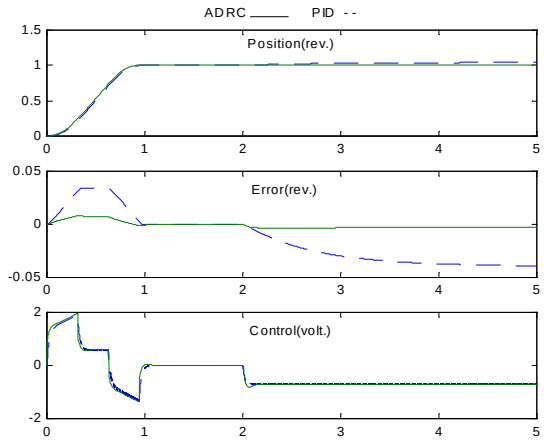

Figure 6 Responses with 20% torque disturbance at 2 second

Validity of the ESO

The key to the success of the ADRC is the ESO, which enables the controller to actively compensate for the changes in the dynamics (inertia) or the disturbances. Mathematically, in the presence of the torque disturbances, $T_d(t)$, the differential equation of the plant can be written as

$$\ddot{y} = (-1.41\dot{y} + 23.2T_d) + 23.2u \qquad (12)$$

The function to be estimated is

$$f(\bullet) = a(t) = -1.41\dot{y} + 23.2T_d - 7.51u \qquad (13)$$

To see the effectiveness of the ESO, we plot $z_3(t)$ against its target a(t) in Figure 7. It is clearly shown that $z_3(t)$ tracks a(t) very closely. This allows the control law in (9) to reduce the plant in (4) to an approximately double integrator, which can be easily controlled with the PD controller in (10).

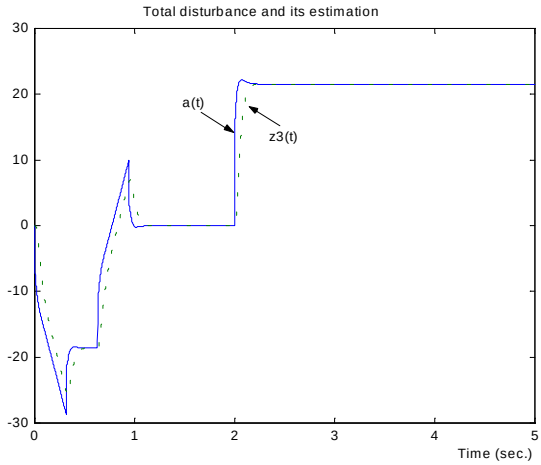

Figure 7 Total disturbance and its estimation

Frequency Domain Disturbance Rejection Characteristics

A common criteria used by control engineers to compare disturbance rejection properties of different control systems is the frequency response. Here, we are interested in two types of disturbance: the position disturbance Y_d and torque disturbance T_d. The frequency response properties of the disturbance rejection are obtained by injecting a sinusoidal signal as the disturbance and observe the induced position signal, particularly its amplitude and phase. The test is repeated at various frequencies until a complete frequency response plot is obtained.

The position and torque disturbance rejection curves are illustrated in Figure 8 and Figure 9, respectively. In both plots, the ADRC betters PID by about 20 dB within the controller bandwidth, which is consistent with the simulation results shown earlier. Note that Figure 8 is also known as the sensitivity function which indicates how sensitive the system is to dynamic (parametric) changes. This helps to explain why the ADRC performed better in simulation when the inertia was doubled.

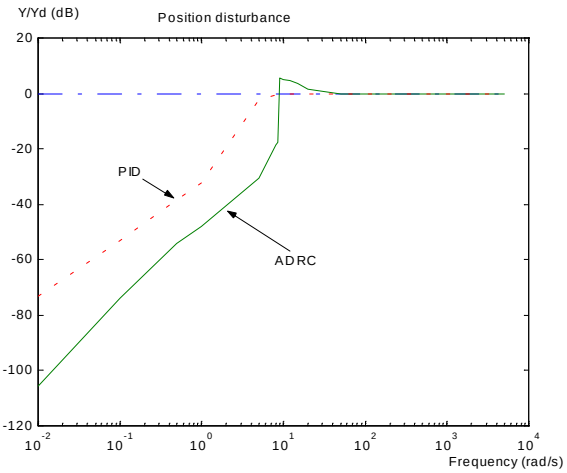

Figure 8 Magnitude of the frequency response from position disturbance Y_d to Y

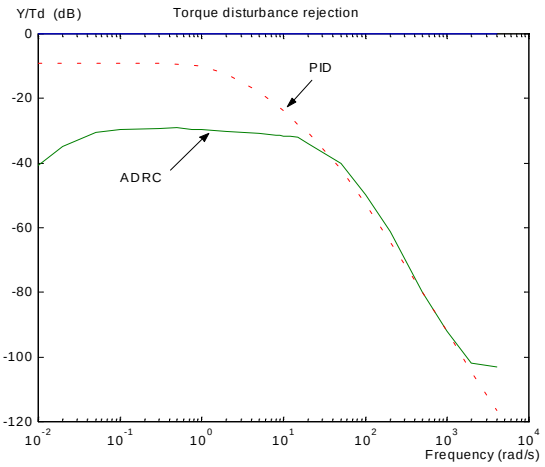

Figure 9 Magnitude of the frequency response from torque disturbance T_d to Y

V. Experimental Results

5.1 Experimental Setup

The experimental setup includes a PC based control platform and a DC brushless servo system made by ECP (Model220) [6]. The servo system includes two motors, one as an actuator, the other as the disturbance source; a power amplifier, and an encoder which provides the position measurement. The inertia, friction, and backlash are all adjustable, making it convenient to test the control algorithms. A Pentium 133 MHz PC running in DOS is programmed as the controller. It contains a data acquisition board for digital to analog conversion and a counter board to read the position encoder output in the servo system. The sampling frequency is 1 KHz.

As shown in Figure 10, the PC performs the position control of the load disc. The position signal is read into the microcomputer via the counter board and the control signals are outputted to the motor drive via DAC. The PID and ADRC control algorithm are written in C language. As a precaution, the output of the controller is limited to ±3.5V. It was also discovered that the drive system has a dead zone of ±0.5V.

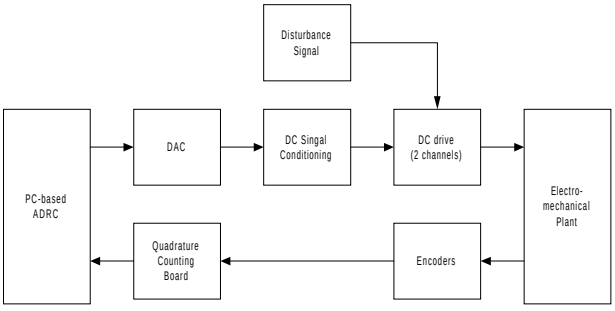

Fig. 10 A diagram for DC brushless servo system

The transfer function from the control signal (voltage command to the power amplifier) to the position of the load is modeled approximately as in (11). In the nominal case, 4 brass weights are placed on the load disc, each of 0.2 Kg, 6.6 cm from the center of the load disk. Initially, no friction, disturbance or backlash is intentionally added. The nominal set point is one revolution.

5.2 Experimental Results and Discussion

To verify the effectiveness of the ADRC, a series of experiments were carried out. The response of the nominal system is plotted in Figure 11. Figure 12 illustrates how the estimate $z_3(t)$ follows its target $\hat{a}(t)$. Here $\hat{a}(t)$ is similarly computed as in (13) but because of the uncertain factors in the hardware setup, such as nonlinearity, disturbances, and dead zone, $\hat{a}(t)$ is only a rough estimate of the real a(t). This helps to explain the discrepancies on Figure 12. Over all, the hardware response is quite close to the that of the simulation.

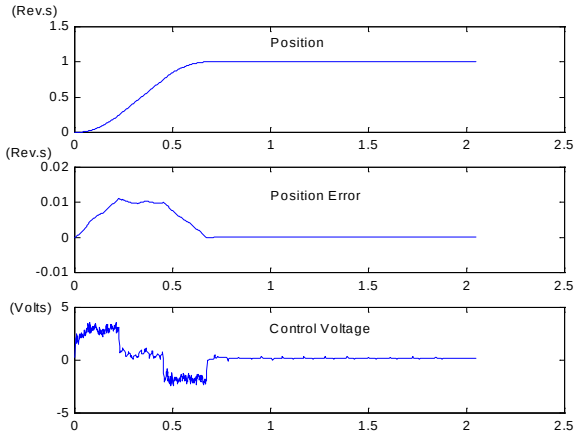

Figure 11 Test Data of the ADRC Servo System

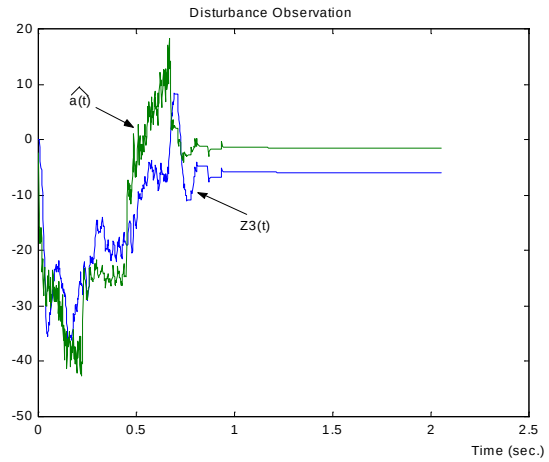

Figure 12 Performance of the ESO

Robustness

To investigate the robustness of the ADRC, the following tests are performed individually:

- Change of setpoint to from 1 to 10 revolutions

- Increase the inertia by 100% (adding two .7 Kg weights to the disc at radius of 7.5 cm)
- Increase the friction significantly by adjusting the rubbing screw in the test setup.
- Introduce 30% torque disturbance (.129 N.m.) using the disturbance motor.

For comparison reasons, both PID and ADRC are tested for each scenario and the results are evaluated in terms of overshoot, setting time, steady state error and the root-mean-square error, defined as:

$$L(e) = \sqrt{\frac{\sum_N (v_1(t) - y(t))^2}{N}} \qquad (12)$$

The results of these tests are listed in Table 1. In general, ADRC outperforms PID by a large margin. It proves to be a much more robust control scheme.

Table 1. Experimental results with ADRC and PID schemes

		Over-Shoot (%)	Settling Time (2% vs one rev.) (sec.)	Steady State Error (rev)	L(e) (rad.)
ADRC	**Nominal Case**	0.00	0.615	6.87×10^{-4}	0.029
	10 Rev.	0.00	2.45	3.80×10^{-3}	0.116
	Load Added	0.30	0.858	1.25×10^{-4}	0.024
	Friction Exerted	0.00	0.625	4.13×10^{-3}	0.037
	30% of T_{max} (0.129 N.m) Disturbance	N/A	0.19	4.13×10^{-3}	0.030
PID	**Nominal Case**	0.20	0.639	1.87×10^{-4}	0.066
	10 Rev.	0.34	2.43	1.86×10^{-2}	0.216
	Load Added	0.98	0.872	5.31×10^{-3}	0.089
	Friction Exerted	0.00	0.669	1.61×10^{-2}	0.128
	30% of T_{max} (0.129 N.m) Disturbance	N/A	2.11	4.69×10^{-2}.	0.196

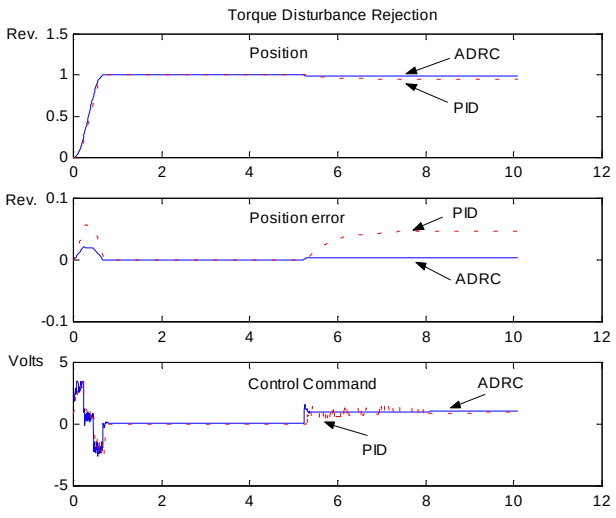

Figure 13 ADRC and PID responses to torque disturbance

Disturbance Rejection

To investigate the disturbance rejection feature of the ADRC algorithm, a step torque disturbance is applied using the second motor in the servo system. It occurs after the system reaches the steady state, as shown in Figure 13. Once again, the ADRC handles it very well. Comparing the ADRC to PID, the position output recovers from this disturbance ten times faster and the resulting steady state error is ten times smaller, as shown in Table 1. This is quite consistent with the previous frequency domain analysis.

VI. Conclusions

A motion control concept is proposed. Its validity and superiority over the existing PID controller are demonstrated in simulation, frequency response analysis, and hardware tests. We believe this to be a promising new technology for industrial applications because 1) it's intuitive; 2) it does not require an explicit model of the plant; 3) it is inherently robust. For practicing engineers familiar with PID, the new method can be viewed as a integrator-less PID where the controller is a PD and the integration effects come from the dynamically compensated plant. In addition to the PID and classical control theory, this new approach perhaps gives control practitioners another alternative. The initial success also provides researchers with a new direction in developing truly robust control design methodology.

Acknowledgement:

The authors would like to express their gratitude to Prof. Jingqing Han for his valuable insight and suggestions.

References

[1] George Ellis, "Control System Design Guide", 2nd Edition, Academic Press, 2000.

[2] Reliance Motion Control Inc., DC Motors, Speed Controlls, Servo Systems, The Electro-Craft Engineering Handbook, 5th Edition.

[3] Jacob Tal, "Motion Control Systems", The Control Handbook. Editor Williams S. Levine, pp. 1382-1386, CRC Press and IEEE Press, 1995.

[[4] Dave Rapini, "New Directions In Motion Control", Motion Control, Jan./Feb. 1999, pp.37-38.

[5] B. Armstrong and C. Canudas de Wit, "Friction Modeling and Compensation", The Control Handbook. Editor Williams S. Levine, pp. 1369-1382, CRC Press and IEEE Press, 1995.

[6] Manual for Model 220 Industrial Emulator/Servo Trainer, Educational Control Products, 5725 Ostin Avenue, Woodland Hills, CA 91367, 1995.

[7] Jingqing Han, "Nonlinear State Error Feedback Control". Control and Decision (Chinese), Vol.10, No.3, Nov., 1994, P221-225.

[8] Zhiqiang Gao, Huang Yi, and Jingqing Han "An Alternative Paradigm for Control System Design", to be presented at the IEEE 2001 Conference on Decision and Control.